Reconstructing Surface EMG from Scalp EEG during Myoelectric Control of a Closed Looped Prosthetic Device

Andrew Y. Paek, *Student Member, IEEE*, Jeremy D. Brown, *Student Member, IEEE*, R. Brent Gillespie, *Member, IEEE*, Marcia K. O'Malley, *Member, IEEE,* Patricia A. Shewokis, *Member, IEEE*, and Jose L. Contreras-Vidal, *Senior Member, IEEE*

Abstract— **In this study, seven able-bodied human subjects controlled a robotic gripper with surface electromyography (sEMG) activity from the biceps. While subjects controlled the gripper, they felt the forces measured by the robotic gripper through an exoskeleton fitted on their non-dominant left arm. Subjects were instructed to identify objects with the force feedback provided by the exoskeleton. While subjects operated the robotic gripper, scalp electroencephalography (EEG) and functional near infrared spectroscopy (fNIRS) were recorded. We developed neural decoders that used scalp EEG to reconstruct the sEMG used to control the robotic gripper. The neural decoders used a genetic algorithm embedded in a linear model with memory to reconstruct the sEMG from a plurality of EEG channels. The performance of the decoders, measured with Pearson correlation coefficients (median r-value = 0.59, maximum r-value = 0.91) was found to be comparable to previous studies that reconstructed sEMG linear envelopes from neural activity recorded with invasive techniques. These results show the feasibility of developing EEG-based neural interfaces that in turn could be used to control a robotic device.**

I. INTRODUCTION

Recent brain machine interface (BMI) research has examined the feasibility of decoding surface electromyography (sEMG) from neural activity extracted with invasive recording techniques [1–4] and noninvasive modalities [5], [6]. Decoding sEMG presents an interest in the field as it provides a direct application to BMI that uses functional electric stimulation (FES) where peripheral muscles are stimulated from external electrical signals [1], [4]. It also provides a wider repertoire of control schemes that can be used to control peripheral hardware where the kinetics (such as torque) can be controlled directly with neural activity as opposed to controlling the kinematics (such as

limb position or joint angle) [1]. There is also a possibility that brain activity may be more correlated to muscle activity as opposed to limb kinematics, which could lead to more reliable control.

Here we demonstrate the feasibility of reconstructing sEMG activity from scalp EEG signals in the delta band (.01 - 1Hz) with a linear decoder with memory (Wiener filter). This strategy is derived from our previous studies, where we found reasonable success in predicting limb kinematics from delta band EEG activity using linear decoders based on the observations that delta band EEG activity is modulated in amplitude with kinematics [7–9].

In this paper we expand upon our previous work where we designed a closed loop prosthetic device that implemented force feedback [10]. This device featured a robotic gripper that was controlled by the subject's bicep EMG and an exoskeleton which provided forces measured by the robotic gripper to the subject. The force feedback in the prosthetic device was found to significantly improve the subjects' ability to discriminate objects of various stiffness [10]. While previous work was primarily aimed to investigate if force feedback improved myoelectric prosthesis control, EEG was also collected in order to study changes in neural activity due to the presence of force feedback. Since the EMG used in the prosthesis directly reflected the user's movement intentions, it was of interest to observe if the EEG collected in the study could reconstruct the EMG, demonstrating the feasibility in operating the robotic gripper with EEG as a BMI. Thus, the goals of this study were to develop a neural decoder based on scalp EEG to reconstruct the EMG used in the control of the robotic gripper and to investigate if the presence of force feedback influenced the reconstructions.

II. METHODS

A. Instrumentation and Behavioral Task

Seven healthy able-bodied human subjects participated and gave informed consent for the following study. Due to technical issues of synchronizing data, the data presented herein reflects that of five subjects. The study called for subjects to control a robotic gripper through EMG signals recorded from the biceps brachii. As the subjects controlled the robotic gripper, two single axis load cells (Transducer Techniques LSP-1) on the tips of the gripper measured how much force was exerted on the gripper due to the gripping action. This force was displayed as an extension torque through a motorized exoskeleton that was fitted on the subject's left arm. As the robotic gripper grasped the object with higher forces, the subject experienced a greater extension torque about the elbow through the exoskeleton.

A. Y. Paek is with the Department of Electrical and Computer Engineering, University of Houston, TX 77004, USA (e-mail: aypaek@uh.edu).

J. L. Contreras-Vidal is with the Department of Electrical and Computer Engineering and the Department of Biomedical Engineering, University of Houston, TX 77004, USA (e-mail:, jlcontreras-vidal@uh.edu).

J. D. Brown and R. B. Gillsepie are with the Department of Mechanical Engineering, University of Michigan, MI 48109, USA (e-mail: jdelaine@umich.edu, brentg@umich.edu).

M. K. O'Malley is with the Department of Mechanical Engineering and Materials Science, Rice University, TX 77005, USA (e-mail: omalleym@rice.edu).

P. A. Shewokis is with the Nutrition Sciences Department in the College of Nursing and Health Professions and a joint appointment in the School of Biomedical Engineering, Science and Health Systems, Drexel University, 19104, Philadelphia, PA., USA (e-mail: pas38@drexel.edu).

Fig. 1 shows the robotic gripper and the exoskeleton. Further technical details of the closed loop prosthetic device can be found in [10].
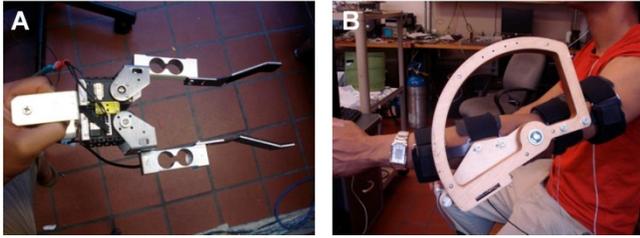

Figure 1. A) Photograph of the robotic gripper that was controlled by the subjects in the study. B) Photograph the exoskeleton which provided force feedback about the elbow to the subject.

Subjects were instructed to use the robotic gripper to grasp three objects of various stiffnesses that were presented randomly. The objects and the gripper were visually hidden from the subjects while they performed the behavioral task. After the subjects squeezed the objects, they were instructed to guess which object was being squeezed. Each object was presented 10 times, which resulted in 30 trials. While the subjects performed this task, neural activity was recorded simultaneously with scalp EEG (Neuroscan Synamps, 64 channel system) and functional near infrared spectroscopy (fNIRs) (Drexel University, 16 sensor strip system). Analysis on the fNIRs data will be published elsewhere.

Four task conditions were applied in this study. In all conditions, the exoskeleton was fitted on the left arm. In the first and second conditions, bicep EMG from the arm that was ipsilateral to the exoskeleton was used to control the robotic gripper. The force feedback was present in the first condition and removed in the second condition. In the third and fourth conditions, bicep EMG from the arm that was contralateral to the exoskeleton was used to control the robotic gripper. The force feedback was removed in the third condition and present in the forth condition.

B. Data Processing

Myoelectric control of the robotic gripper: The linear envelope of the biceps EMG was used to control the robotic gripper. To extract the linear envelope, EMG was rectified and low pass filtered with a cutoff at 0.159 Hz. This linear envelope was used during the recording session for subjects to control the robotic gripper. For the analysis, the linear envelope of the EMG was resampled to 100 Hz and synchronized with the scalp EEG which was also resampled at 100Hz.

Decoding Surface Electromyography from Scalp Electroencephalography: Scalp EEG was preprocessed before it was used to reconstruct the linear envelope of bicep EMG. First, 13 peripheral EEG sensors that were obstructed by the fNIRs sensors were omitted for the rest of the analysis. EEG recordings were then common average referenced to remove the common noise across all the electrodes. Next the EEG signals were high pass filtered at 0.01 Hz with an 8th order Butterworth filter to remove drifts in EEG signal amplitude across the recording session. While decoding studies typically use 0.1 Hz as the high pass cut off frequency, we found that using 0.01 Hz allows the decoder to

perform better. This may occur because EMG envelopes contain significant amount of power below 0.1 Hz due to very slow muscle contractions. The EEG signals were then low pass filtered at 1 Hz with a first order Butterworth filter in order to extract the delta band EEG signals and for the frequency content of the EEG signals to be similar to that of the EMG linear envelope (in the EMG linear envelopes, at least 90% of the power in the power spectral density estimates were found to be below 1 Hz). From the continuous data, trials of EEG and EMG data were extracted from the time duration 2 seconds before and 12 seconds after the onset of movement. The EEG and EMG signals were then resampled at 20 Hz in order to reduce the time needed to further process the data while maintaining the frequency content of the signals. The amplitude of the EEG and EMG signals were then standardized with respect to their means.

The neural decoder used a linear model (Weiner filter) to reconstruct the linear envelope of the EMG activity. The amplitude of the EMG linear envelope was approximated as the weighted sum of the signals of the preprocessed EEG signals. In addition, EEG signals from the past are also added into the approximation. The following equation illustrates this relationship:

$$Y(t) = \sum_{i=1}^{N} \sum_{k=0}^{L} b_{ik} * S_i(t-k) \qquad (1)$$

where $Y(t)$ is the amplitude of the EMG linear envelope at time t, $S_i(t-k)$ is the amplitude of the EEG signal from the i-th electrode (up to N=49 sensors were included) at time $t - k$, k is the time lag in the past (N=6 lags from 0 to 250 milliseconds in 50 millisecond increments were used), and b_{ik} are the coefficients of the linear model. These coefficients were determined by fitting a generalized linear model with the MATLAB *glmfit* function.

The model was trained and validated using leave-one-out (LOO) cross validation. In this scheme, all but one trial was used to train the model. For the trial that remained, the EEG signals were used to reconstruct the EMG based on the model which was trained with the other trials. The reconstructed EMG was low pass filtered at 1 Hz with a first order Butterworth filter. The Pearson's correlation coefficient (r-value) was calculated between the reconstructed EMG and the observed EMG in the trial in order to quantify how well the two trajectories matched each other. This process was repeated so that each and every trial was used to validate the model that was trained with the other trials.

The LOO cross validation was repeated with various combinations of EEG sensors as it was generally found that the inclusion of all EEG sensors did not yield the maximum accuracy of the decoder due to overfitting of data. Since the time needed to test all possible combinations of sensors would have been unwieldy, a genetic algorithm was used to find the optimal set of EEG sensors that maximized performance, where new combinations of EEG sensors were derived from previous EEG sensor combinations that performed well.

To investigate how the neural decoder was influenced by the presence of force feedback, the LOO cross validation was performed within each of the four conditions mentioned above. LOO cross validation was also performed with trials

5603

across all conditions to determine if a neural decoder can be trained such that it can reconstruct the EMG across various conditions. Lastly, the neural decoder was also trained with all trials from one condition and tested with all trials in each of the four conditions to assess the neural decoder's generalizability between conditions.

III. RESULTS

The neural decoder performed similarly across all four conditions as shown in Fig. 2. The distributions of the accuracies were negatively skewed, indicating that the performance of our decoder usually had more instances of good decoding performance and rare instances of poor
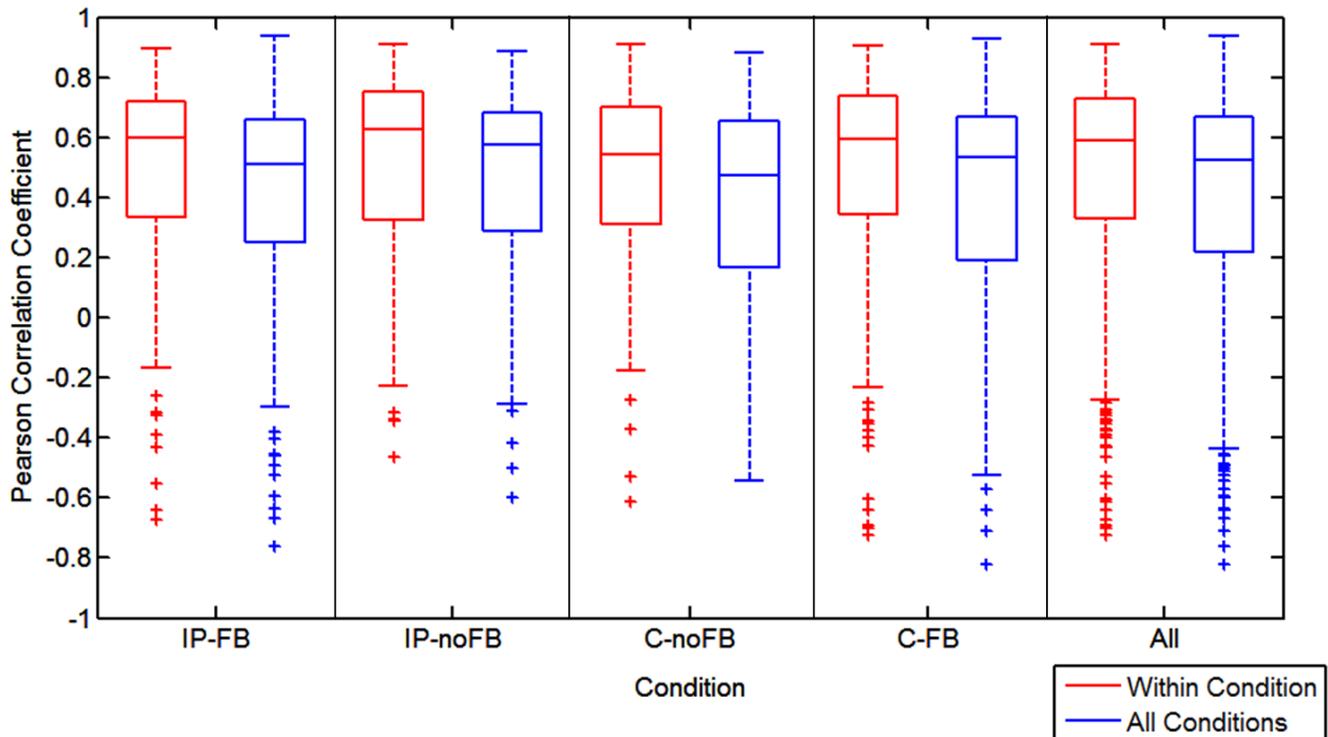

Figure 2. Boxplots of decoding accuracies across all five subjects. Outliers are shown as plus symbols. Labels "IP" and "C" correspond to conditions when the exoskeleton was respectively placed ipsilateral and contralateral to the arm which controlled the robotic gripper. "FB" and "noFB" correspond to conditions when the exoskeleton respectively provided force feedback or did not provide feedback. Red boxplots correspond to accuracies where the neural decoder was trained and tested with data from only one condition. Blue boxplots correspond to accuracies where the neural decoder was trained and tested with data simultaneously from all conditions. Median values for each boxplot are as follows: 0.60, 0.51, 0.62, 0.58, 0.54, 0.47, 0.60, 0.53, 0.59, 0.53.
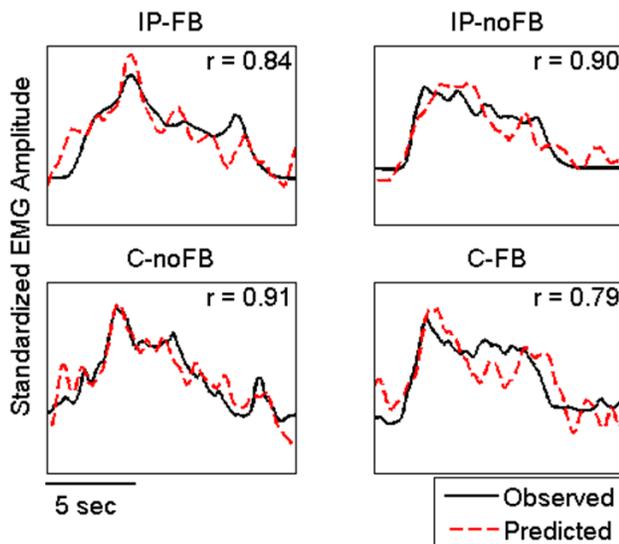

Figure 3. Best examples from subject 1 of reconstructed (dotted red line) and observed (solid black line) of the EMG linear envelopes used to control the robotic gripper. The correlation coefficient between the observed and predicted linear envelopes are shown in the upper right of each plot. Labels correspond to the same conditions indicated by Fig. 2.
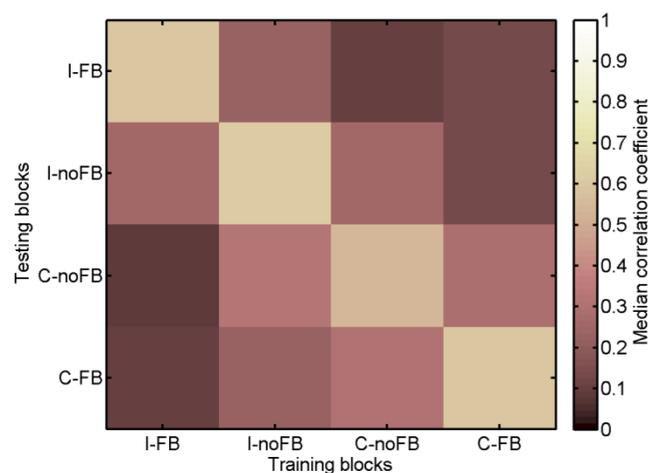

Figure 4. Plot of median correlation coefficients of the decoder when trained with one condition and tested on others. Columns indicate conditions used to train the decoder while rows indicate conditions used to test the decoder. Values on the main diagonal correspond to medians from the LOO cross validation within each condition. Labels correspond to the same conditions indicated by Fig. 2.

decoding. It was speculated that the trials with poor reconstructions occurred due to EEG artifacts (such as eye blinks). When the neural decoder was trained and tested within each condition, the decoding accuracies yielded a median correlation coefficients of r = 0.59 and a maximum of r = 0.91. When the neural decoder was trained with data from all conditions, the decoder appeared to perform slightly worse in each condition, yielding a median correlation coefficient of r = 0.53 and a maximum r = 0.94.

In the best examples of the reconstructions, the predicted EMG linear envelopes generally follows the same trajectory as the observed EMG envelopes as shown in Fig. 3. We note how the observed EMG envelopes usually contained single muscle contractions that persisted for several seconds.

When the neural decoder was trained with data within one condition and tested with trials from other conditions, the neural decoder performed the best when tested with trials from the same condition and considerably worse on the others as shown in Fig. 4.

IV. DISCUSSION

Our performance with the decoding of EMG was comparable to that of previous studies that have reconstructed EMG linear envelopes from invasive neural recording techniques. Table 1 reviews the decoding accuracies of previous literature where EMG was reconstructed from neural activity recordings. The results from this study support the feasibility of developing BMI systems with noninvasive scalp EEG. Our results indicate that within each task condition, the neural decoder was able to reconstruct the EMG at similar accuracies. However, training the neural decoder with one task condition and testing it in other conditions yielded poorer accuracies, indicating that training with one condition does not make the neural decoder generalizable across different conditions. It suggests that the task in each condition yields fairly unique neural signatures in terms of which arm was used to control the robotic gripper and on processing force feedback. However, we also found that training the neural decoder with data from all conditions yielded only a marginal reduction in decoding accuracies, which may suggest that similarities in the neural signature exist across all conditions that can be employed for predicting EMG in various conditions.

Despite the small differences in the decoder's performance across the four conditions, it is very likely that each condition would have yielded unique EEG signatures. Further work will investigate how each condition creates differences in spatial areas that are correlated to EMG activity. Such analysis would investigate how often each EEG sensor was chosen in the genetic algorithm and calculate on a trial by trial basis how correlated each sensor was to the EMG.

Another aspect of the study that remains to be investigated is how subjects learned to use the force feedback to identify objects. It is expected that this learning effect would change the neural activity related to the EMG. This could introduce inconsistencies in the relationship between scalp EEG and EMG throughout the training data, which could influence the neural decoder's performance in reconstructing EMG.

TABLE I. REVIEW OF EMG RECONSTRUCTION STUDIES

Behavioral Task	Decoding accuracy	Notes	Ref.
Reach to grasp, isometric wrist movements	VAF = 0.67	M1 spike and Local Field Potentials, 5 Hz EMG LE*, monkeys	[1]
Reach to grasp	r = 0.69	M1 neuron spikes, 40 ms average windowed rectified EMG, monkeys	[2]
Center out reach	R^2 = 0.65	M1/PMd neuron spikes, 25 ms Gaussian filtered rectified EMG, monkeys	[3]
Stand and squat	R^2 = 0.74	M1 Spike recordings, 4 Hz EMG LE*, monkeys	[4]
Isometric wrist movements	R^2 = 0.47	fMRI BOLD response, integrated EMG convolved with HRF, humans	[5]
Isometric wrist flexion/extension	R^2 = 0.71 (source current) R^2 = 0.55 (electrode recordings)	Scalp EEG, localized source currents, 2.2 Hz EMG LE*, humans	[6]
Prosthesis control with biceps contraction	r = 0.59	Scalp EEG, 0.167 Hz EMG LE*, humans	Current Study

* Pertains to the low pass filter cut off for linear envelopes (LE)

REFERENCES

[1] R. D. Flint, C. Ethier, E. R. Oby, L. E. Miller, and M. W. Slutzky, "Local field potentials allow accurate decoding of muscle activity.," *J neurophysiol*, vol. 108, no. 1, pp. 18–24, Jul. 2012.

[2] D. Song, P. Hendrickson, V. Z. Marmarelis, J. Aguayo, J. He, G. E. Loeb, and T. W. Berger, "Predicting EMG with generalized Volterra kernel model.," *Conf Proc IEEE Eng Med Biol Soc*, vol. 2008, pp. 201–4, Jan. 2008.

[3] Z. Rivera-Alvidrez, R. S. Kalmar, S. I. Ryu, and K. V Shenoy, "Low-dimensional neural features predict muscle EMG signals.," *Conf Proc IEEE Eng Med Biol Soc*, vol. 2010, pp. 6027–33, Jan. 2010.

[4] H. Zhang, C. Ma, and J. He, "Predicting lower limb muscular activity during standing and squatting using spikes of primary motor cortical neurons in monkeys.," *Conf Proc IEEE Eng Med Biol Soc*, vol. 2010, pp. 4124–7, Jan. 2010.

[5] G. Ganesh, E. Burdet, M. Haruno, and M. Kawato, "Sparse linear regression for reconstructing muscle activity from human cortical fMRI.," *NeuroImage*, vol. 42, no. 4, pp. 1463–72, Oct. 2008.

[6] N. Yoshimura, C. S. Dasalla, T. Hanakawa, M.-A. Sato, and Y. Koike, "Reconstruction of flexor and extensor muscle activities from electroencephalography cortical currents.," *NeuroImage*, vol. 59, no. 2, pp. 1324–37, Jan. 2012.

[7] T. J. Bradberry, R. J. Gentili, and J. L. Contreras-Vidal, "Reconstructing three-dimensional hand movements from noninvasive electroencephalographic signals.," *J neurosci*, vol. 30, no. 9, pp. 3432–7, Mar. 2010.

[8] A. Presacco, R. Goodman, L. Forrester, and J. L. Contreras-Vidal, "Neural decoding of treadmill walking from noninvasive electroencephalographic signals.," *J neurophysiol*, vol. 106, no. 4, pp. 1875–87, Oct. 2011.

[9] A. Presacco, L. Forrester, and J. L. Contreras-Vidal, "Decoding Intra-Limb and Inter-Limb Kinematics During Treadmill Walking From Scalp Electroencephalographic (EEG) Signals," *IEEE Trans Neural Syst Rehabil Eng*, vol. 20, no. 2, pp. 212–219, 2012.

[10] R. B. Gillespie, J. L. Contreras-Vidal, P. a Shewokis, M. K. O'Malley, J. D. Brown, H. Agashe, R. Gentili, and A. Davis, "Toward improved sensorimotor integration and learning using upper-limb prosthetic devices.," *Conf Proc IEEE Eng Med Biol Soc*, vol. 2010, pp. 5077–80, Jan. 2010.